Available online at www.sciencedirect.com
ScienceDirect
Journal of Catalysis 249 (2007) 93–101
JOURNAL OF CATALYSIS
www.elsevier.com/locate/jcat

Palladium-catalyzed liquid-phase hydrogenation/hydrogenolysis of disulfides

Ekaterina K. Novakova [a,b], Leanne McLaughlin [a], Robbie Burch [a], Paul Crawford [a], Ken Griffin [b], Christopher Hardacre [a,*], Peijun Hu [a], David W. Rooney [a]

[a] *CenTACat and School of Chemistry and Chemical Engineering, Queen's University Belfast, Belfast BT9 5AG, Northern Ireland, UK*
[b] *Johnson Matthey Catalysts, Orchard Road, Royston SG8 5HE, UK*

Received 31 January 2007; revised 30 March 2007; accepted 3 April 2007

Abstract

For the first time, the hydrogenation/hydrogenolysis of a range of disulfides has been achieved over a supported palladium catalyst using hydrogen under relatively benign conditions. These unexpected results demonstrate that it is possible to avoid the poisoning of the catalyst by either the nitrogen-containing groups or the sulfur species, allowing both efficient reaction and recycling of the catalyst under the proper conditions (e.g., at low temperatures). A slight loss in activity was found on recycling; however, the catalyst activity can be recovered using hydrogen pretreatment. The reaction mechanism for the hydrogenolysis and hydrogenation of *ortho*-, *meta*-, and *para*-dinitrodiphenyldisulfide to the corresponding aminothiophenol has been elucidated. Density functional theory calculations were used to investigate the adsorption mode of the dinitrodiphenyldisulfides; a clear dependence on adsorption geometry was found regarding whether the molecule is cleaved at the S–S bond before the reduction of the nitro group or vice versa. This study demonstrates the versatility of these catalysts for the hydrogenation/hydrogenolysis of sulfur-containing molecules, which normally are considered poisons, and will extend their use to a new family of substrates.

Keywords: Catalyst; Palladium; Hydrogenation; Hydrogenolysis; Heterogeneous; Sulfide; Nitro; Amine

1. Introduction

Thio-products, such as mercaptans, sulfides, polysulfides, sulfones, thioacids, and thioesters, have an increasing share in the industrial production of pharmaceuticals, agrochemicals, cosmetics, and petrochemical products. The synthesis of mercaptans is particularly important, because these are often used as precursors in the production of other thio-compounds. Currently, aliphatic mercaptans are produced via the direct thiolation of alcohols with H_2S over alkali metal catalysts in yields >95% [1]. In comparison, the production of aromatic thiols via this method is not efficient, resulting in low yields due to reduced selectivity at the high temperatures needed to achieve viable reaction rates [2]. Current methods for forming benzenethiol derivatives include the reduction of sulfonic acids [3] or their sulfonyl chlorides [4] with phosphorus or hydrogen, produced in situ in the presence of a mineral acid and a metal. Although these reactions are highly selective, large amounts of phosphoric acid and/or metal chloride waste are also produced.

One possible alternative route to the production of aromatic mercaptans is through reductive cleavage of the corresponding disulfides. This reaction has been extensively studied for the cleavage of S–S bonds in proteins to change their tertiary structure. This is conventionally achieved to form thiols and thiolates using stoichiometric nucleophilic reagents, such as hydrides in the form of $NaBH_4$ [5]; phosphorous compounds, such as triphenylphosphine [6]; or hydrazine derivatives, such as semicarbazide [7]. Few catalytic processes for the reduction of S–S bonds have been reported due to the potential strong chemisorption of sulfur-containing molecules and their ability to poison metal surfaces. To date, Calais et al. have reported the only process for cleaving a range of substituted diphenyldisulfides over sulfided Ni–Mo/Al_2O_3 catalyst [8,9]. The choice of cata-

* Corresponding author. Fax: +44 28 9097 4687.
E-mail address: c.hardacre@qub.ac.uk (C. Hardacre).

0021-9517/$ – see front matter
doi:10.1016/j.jcat.2007.04.002

lyst was thought to be important, because it is commonly used for the gas-phase hydrotreatment and desulfurization in petroleum refining. This catalyst is able to catalyze hydrogenation and carbon-heteroatom hydrogenolysis while being highly resistant to sulfur poisoning. In this study, selective reduction of the diphenyldisulfide was achieved at 160 °C and 3 bar hydrogen [8]. After introducing *para*-substituents, such as methyl, amine, chloro, nitro and hydroxyl groups, a reduction in the rate of reaction was observed. This reduced activity was particularly evident for 4,4′-dinitrodiphenyldisulfide, where up to 200 °C and 10 bar hydrogen were required for the reaction to reduce both the nitro group and disulfide linkage to form 4-aminothiophenol. Using theoretical models, the behavior of 4-nitrodiphenyldisulfide was explained by a difference in the adsorption geometry. The molecule was thought to adsorb predominantly *via* the nitro groups, forcing the S–S bond away from the surface and reducing the likelihood of reductive cleavage. Such an effect also has been reported for other hydrogenation reactions [10]. In contrast to the reaction with hydrides, where the rate increased with decreasing aromatic electron density [5], for the catalyzed reactions, no correlation with the electronic property of the reactant was observed.

In the present study, we investigated the hydrogenation/hydrogenolysis of $–NO_2–$, $–NH_2–$, $–CH_3–$, and $–OCH_3$-substituted diphenyldisulfide as well as dibenzyldisulfide and dimethyl- and dibutyldisulfides using a carbon-supported platinum group metal (PGM) catalyst (Fig. 1). Whereas platinum and palladium are commonly used for the hydrogenation of a wide range of substrates, PGM is very susceptible to poisoning by sulfur [10–23]. This is thought to be particularly problematic on palladium; consequently, fewer studies on this have been reported. Sulfur poisoning on metals is thought to be a combination of both geometric and electronic effects, giving rise to changes in short-range and long-range interactions. The geometric effect is related to the length of the carbon chain attached to the S-atom anchored to the surface; this is, the larger the poison molecule, the larger the area of the surface blocked [11,24]. In contrast, the electronic effect results in changes in the electron density of the catalyst surface as a result of the strong covalent bonds between the metal atoms and the sulfur [19]. This is used in some cases to tune the reaction selectivity by exposing the catalyst to either dimethyldisulfide or thiophene [25,26]. For example, dimethyldisulfide is decomposed to H_2S under hydrogenation conditions at 200 °C, which then adsorbs and modifies the catalyst surface [22]. Here we report on the feasibility of using PGM catalysts for the hydrogenation/hydrogenolysis of a range of aromatic and aliphatic disulfides under mild reaction conditions.

2. Experimental

2.1. Materials

All experiments were carried out using nominal 10 wt% Pd catalyst supported on charcoal as provided by Johnson Matthey. Metal analysis of the catalyst using a Perkin–Elmer Optima 4300 ICP-OES analysis showed a Pd content of 9.93 wt%. The catalyst had a BET surface area of 1335 $m^2\,g^{-1}$ and a Pd surface area of 25 $m^2\,g^{-1}$ measured by CO chemisorption, along with a particle size of <38 μm. In all cases, the catalyst was used as received with no pretreatment. All tested disulfides were purchased from Aldrich with >97% purity. The catalyst was characterized by powder XRD before and after reaction at room temperature using a PANalytical X'PERT PRO MPD X-ray diffractometer with CuK_α radiation.

2.2. Typical reaction and recycle procedure

All reactions were carried out in a high-pressure 300-cm^3 Parr autoclave modified with baffles and a gasifying stirrer to ensure good mixing. Unless stated otherwise, 5 mmol substrate in 200 cm^3 THF was placed in the reactor with 200 mg of catalyst and heated to 75 °C under N_2 before the desired pressure of hydrogen was introduced. The speed of the stirrer rotation was

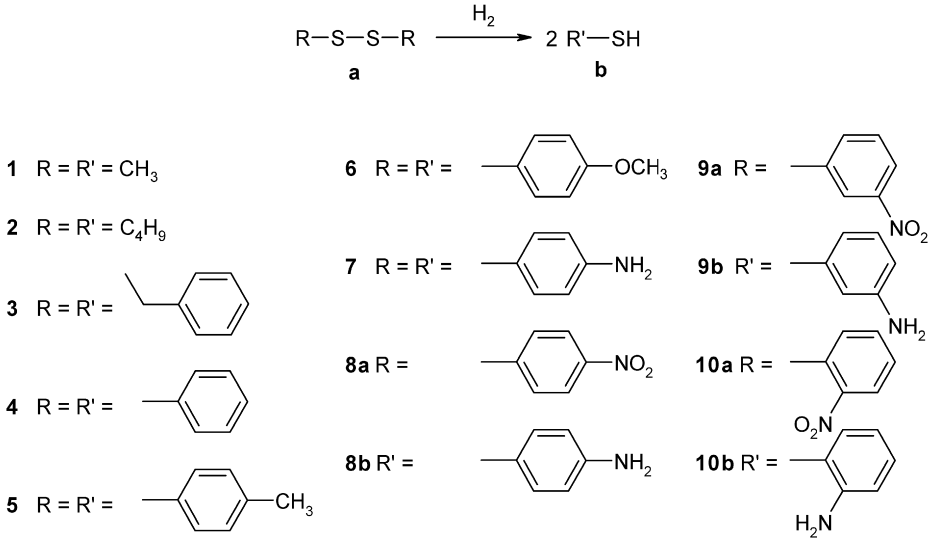

Fig. 1. Reaction scheme and notation for the disulfides used in this study.

maintained at 850 rpm to ensure that the reaction was chemically controlled and free of external mass transfer limitations. The hydrogen was supplied through a delivery system to guarantee a constant pressure of the gas in the autoclave throughout the reaction. Samples were withdrawn at regular intervals and analyzed in an offline Perkin–Elmer Clarus 500 gas chromatograph fitted with a ZB-5 capillary column. The gas chromatography (GC) temperature program ranged from 35 to 250 °C at a heating rate of 6–10° min^{-1} depending on the disulfide used. For recycling reactions, the catalyst was filtered, washed with neat solvent, dried under ambient conditions, and used without further pretreatment. For all reactions, the temperature was below the decomposition temperature of the disulfide as measured by TGA; for example, the 4,4′-dinitrodiphenyldisulfide was found to decompose at 230 °C. The initial rate data was determined by the rate of conversion of the substrate at time = 0 with respect to the surface area of the palladium.

2.3. Adsorption studies

One-component solutions of the starting material, intermediates, and the final product were stirred with a fixed amount of catalyst and charcoal support (0.1 g) for 24 h at 20 °C. A comparison of the solution before and after contact with the catalyst over a concentration range of 0.005–0.05 M for each component was used to determine the adsorption isotherm. GC was used to analyze the solutions after the catalyst was filtered.

2.4. Calculation details

All density functional theory (DFT) calculations were performed using the SIESTA package [27], which uses Troullier–Martins norm-conserving pseudopotentials and numerical atomic orbital basis functions [28]. The generalized gradient approximation exchange–correlation functional of Perdew et al. was used, as was a double zeta with a polarization quality basis set [29]. The orbital-confining cutoff radii were determined from an energy shift of 0.01 eV, and the grid point spacing on the real space density grid corresponded to a cutoff energy value of 150 Ry. A Nose thermostat was used in the finite-temperature molecular dynamics runs, with an initial temperature of 150 K and a target temperature of 250 K. The duration of the time step was set to 0.3 fs.

3. Results and discussion

A range of disulfides were tested at 5 and 50 bar hydrogen pressure using 10 wt% Pd/C. Fig. 2 summarizes the initial rates of reaction. In all cases, the substrates were converted to the corresponding thiol with high selectivity (albeit after extended reaction times in some cases). For the dinitrodiphenyldisulfide derivatives (**8a**, **9a**, **10a**), reduction of the nitro group also was also observed. The rate could be increased by operating at higher temperatures; for example, using diglyme as the solvent, the reaction of **8a** at 160 °C and 50 bar H_2 pressure showed an initial rate of 0.45 μmol s^{-1} $m_{Pd}{}^{-2}$, compared

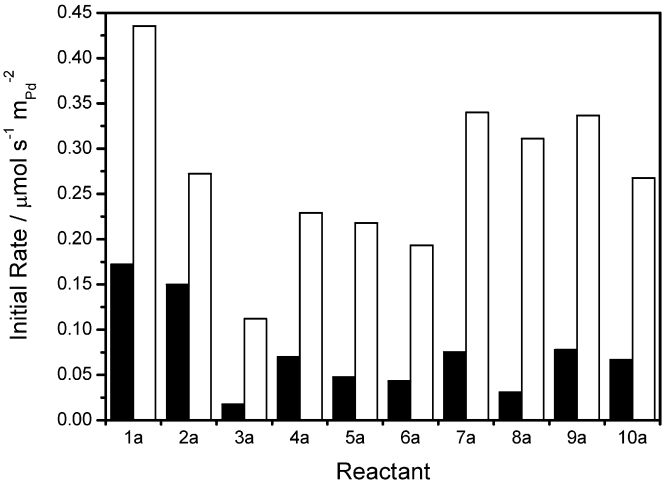

Fig. 2. Initial reaction rate for the hydrogenation/hydrogenolysis of the disulfides (**1a**–**10a**) at 5 bar (■) and 50 bar (□) hydrogen and 75 °C in THF using a Pd:substrate ratio of 1:26.

with 0.30 μmol s^{-1} $m_{Pd}{}^{-2}$ in THF at 75 °C and 50 bar H_2. To eliminate any catalytic effect from the support or thermal decomposition, the blank reaction and a reaction using the carbon support were carried out at 50 bar H_2 pressure and 75 °C. Little reaction was found for the nitro-containing substrates; for example, using **8a**, <4% of the starting material was converted after 6 h of reaction using the carbon support as the catalyst. For the other disulfide substrates, blank reactions in the absence of hydrogen showed no reaction; however, when using 50 bar H_2 in the absence of catalyst for substrates **2a**, **3a**, and **4a**, up to 25% of the starting material was converted over a 6-h period.

3.1. Hydrogenolysis of aliphatic disulfides

The three disulfides studied with aliphatic linkages [dimethyldisulfide (**1a**), dibutyldisulfide (**2a**), and dibenzyldisulfide (**3a**)] exhibited surprisingly high rates of hydrogenolysis. This finding was unexpected, given that **1a**, for example, is often used to poison the most active sites of noble metal catalysts to regulate their selectivity [19]. The mechanism of this sulfur poisoning is thought to involve an initial step in which the sulfur is highly dispersed on the metal surface. At low coverage, the sulfur atoms can change the reactivity of up to 4/5 Pd atoms; however, with increasing coverage the surface becomes completely deactivated [19–21]. Our experiments used a substrate-to-Pd mole ratio of 26:1; this large excess of sulfur in the system carried the potential to completely poison the catalyst surface, yet this did not happen.

Comparing the rates of reaction of these disulfides shows that removing the aromatic ring or decreasing the chain length from butyl to methyl increased the rate. This reduction in rate reflects the increasing cross-section of the disulfide and hence a larger adsorption energy, leading to reduced hydrogen coverage. These results are consistent with the inhibitory effects of sulfur-containing molecules on the hydrogenation of maleic acid reported by Lamy-Pitara et al. [30], who correlated decreased rates of reaction with the size of the additive and its

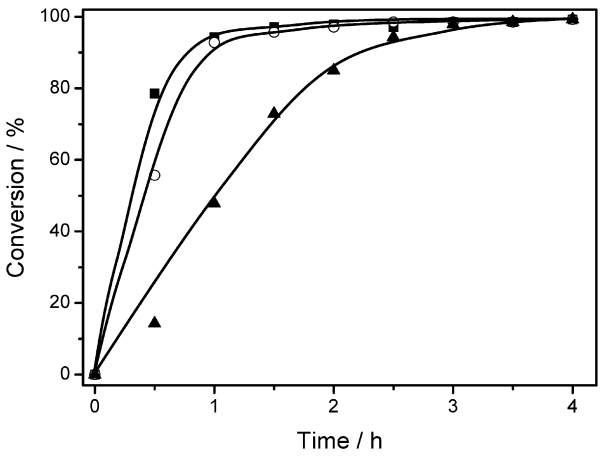

Fig. 3. Comparison of the time variation of the conversion of the aliphatic disulfides **1a** (■), **2a** (○), and **3a** (▲) at 50 bar H_2 and 75 °C in THF using a Pd:substrate ratio of 1:26. The lines are to indicate the trends in the data.

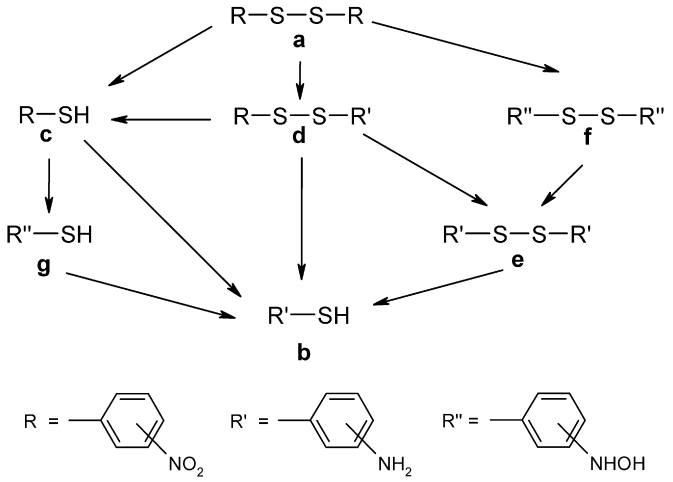

Fig. 4. Reaction pathways for the hydrogenation/hydrogenolysis of 2,2′-, 3,3′-, and 4,4′-dinitrodiphenyldisulfides.

effective surface area on the catalyst [30]. All of the disulfides selectively converted to the corresponding thiols within 5 h.

3.2. Hydrogenation/hydrogenolysis of aromatic disulfides: S–S bond hydrogenolysis

To examine the effect of the aromatic substituent, two families of aromatic disulfides were studied: (**4**, **5**, **6**, **7**, **8a**), that is, *para*-substitution with –H, $–CH_3$, $–OCH_3$, $–NO_2$, and $–NH_2$, and (**8a**, **9a**, **10a**), that is, 2,2′-, 3,3′-, and 4,4′-dinitrodiphenyldisulfide. In agreement with Calais et al. [9], no clear dependence between the electronic properties of the *para*-group was observed with the initial rates of reaction showing $–NH_2 > –NO_2 \gg –H > –CH_3 > –OCH_3$. Interestingly, reasonable rates of reactions were achieved with the nitro-derived disulfides under similar conditions as for the other molecules. This is in contrast to the findings of Calais et al., who reported significantly lower rates of reaction and the need for even more severe conditions for the reduction of nitro-substituted diphenyldisulfide [9].

The initial rates of **4a**–**7a** were significantly higher (by factor of 2) than that of **3a** at any hydrogen pressure and lower than that of **2a**. The only exception was **7a**, which showed a faster reaction rate at 50 bar compared with **2a**. According to the conformational analysis and MO calculations of Calais et al. [9], substituted diphenyldisulfides adsorb with their S–S bond to the surface, whereas the benzene rings are in a perpendicular position. This should result in less metal area covered by the substituted aromatic hydrocarbon and higher rates than the aliphatic disulfides. But we observed the opposite trend, possibly reflecting the possibility of the aromatic rings adsorbing parallel to the surface in the case of PGM catalysts [31].

Interestingly, a much greater difference in the rates at 5–50 bar was found for those disulfides containing aromatic rings compared with the aliphatic disulfides. This may be explained in terms of the adsorption configuration. Whereas at low pressure the molecule lies flat on the surface, at 50 bar the increased competition from the H_2 causes the substrate to undergo a conformational change, freeing up reaction sites and leading to a significant increase in rate.

3.3. Hydrogenation/hydrogenolysis of dinitrodiphenyldisulfides: Reaction mechanism

As well as cleavage of the disulfide bond, the hydrogenation/hydrogenolysis of the dinitrodiphenyldisulfide substrates involves an additional step in order to reduce the two nitro groups. Fig. 4 shows a range of reaction pathways for the reduction of dinitrodiphenyldisulfide to the corresponding aminothiophenol via a number of intermediate products. Two major pathways exist for the formation of aminothiopenol:

Pathway A: Initial cleavage of the S–S bond followed by subsequent reduction of $–NO_2$ to $–NH_2$ directly or via –NHOH.

Pathway B: Reduction of either or both $–NO_2$ groups to $–NH_2$ or –NHOH, followed by cleavage of the S–S bond.

The typical reactant/product composition as a function of time for **8a** is shown in Fig. 5. This type of profile is expected for sequential reactions in which intermediates are desorbed before readsorption and further reaction. At the end of the reaction, the only product present was the desired 4-aminothiophenol (**8b**). With the exception of **8f**, the other intermediates (i.e., **8c**, **8d**, **8e**, and **8g**) were identified by GC-MS and confirmed by injecting standards. The intermediate, **8f**, was identified as an oxime; however, due to an absence of a standard and the low concentration in the reaction medium, it was not possible to determine whether monooxime or (more likely) dioxime was formed.

Although the reaction profile clearly show that both routes occurred for **8a** with the formation of the full range of products and both **8c** and **8d** formed initially, the predominant route to the formation of **8b** was through reduction of **8c**, with **8d** gradually converting into **8f** and **8e** before cleavage occurs. This indicates that pathway A was more facile than pathway B for **8a**. Similar profiles were also observed for the **10a** and **9a** starting materials, with approximately the same rate of conversion found in each case. However, some changes occurred in the proportion of aminothiophenol derived from each pathway.

This is most clearly illustrated by comparing the proportion of diaminodiphenyldisulfide for each of the molecules during the reaction. The maximum amounts of diaminodiphenyldisulfide produced for **8a**, **9a**, and **10a** were 19%, 35%, and 67%, respectively, indicating that the S–S bond became more stable as the nitro group moved closer. This is unlikely to be an electronic effect, given that the *meta*-position is not anomalous, or a steric effect, due to the size of the hydrogen atom.

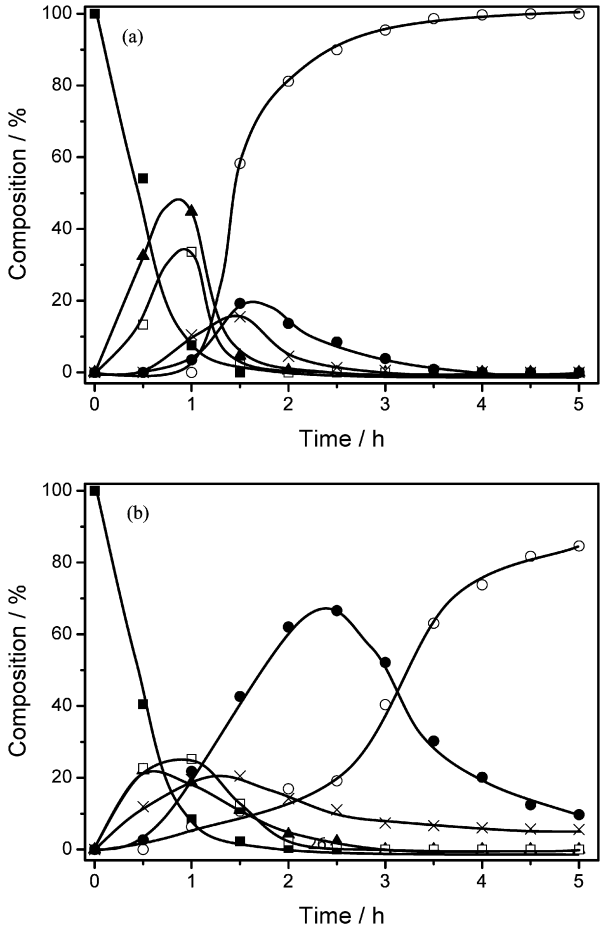

Fig. 5. Reaction composition-time profile for the hydrogenation/hydrogenolysis of (a) 4,4′-dinitrodiphenyldisulfide (**8a**) and (b) 2,2′-dinitrodiphenyldisulfide (**10a**) at 50 bar H_2 at 75 °C in THF using a palladium:substrate ratio of 1:26. Herein, the molecules shown by the notation in Fig. 4 are denoted: **a** (■), **b** (○), **c** (▲), **d** (□), **e** (●), and **f** (×). The lines are to indicate the trends in the data.

To address this disparity in diaminodiphenyldisulfide production, computational studies were performed to ascertain how **8a** and **10a** interact with the catalyst. Molecular dynamics (MD) simulations within the framework of DFT were first performed to investigate the behavior of both the *para*- and *ortho*-substituted disulfides over Pd(111). These simulations suggested that for both iosomers, a flat-lying disulfide adsorption mode was unstable relative to dissociation to monomers; that is, any flat-lying dimer on Pd(111) spontaneously dissociated to its respective monomers. However, further investigation revealed that **10a** could form a stable adsorption geometry by bonding side-on with the surface via the nitro group. This mode of interaction clearly is not available to **8a**.

To determine the relative energetics of each molecule, the adsorption conformations of the resultant monomers and the side-on mode of **10a** established from the MD simulations were optimized until the maximal forces on each atom reached a convergence criteria of 0.05 eV $Å^{-1}$. The optimized adsorption geometries of the *para*- and *ortho*-substituted monomers are shown in Figs. 6a and 6b, respectively, with the side on adsorption mode of **10a** shown in Fig. 6c. The dissociative adsorption energy of **8a** and **10a** and the side-on adsorption energy of **10a** relative to the respective relaxed gas-phase molecules were subsequently calculated and are summarized in Table 1.

The results imply that the adsorption geometry of **10a** is mainly responsible for the difference in the dominant reaction pathways. In the flat-lying state, cleavage of the disulfide before reduction is favored, whereas in the side-on mode of adsorption, the $–NO_2$ groups reduce due to the fact that the S–S bond is not in contact with the surface. In the case of **8a**, rapid cleavage of the S–S bond occurs due to adsorption parallel to the surface. In contrast, in the case of **10a**, the availability of two

Table 1
Comparison of the calculated dissociative adsorption energy of 2,2′-dinitrodiphenyldisulfide (**10a**) and 4,4′-dinitrodiphenyldisulfide (**8a**) following adsorption in a flat-lying geometry with the chemisorption energy of the side-on adsorption mode of 2,2′-dinitrodiphenyldisulfide (**10a**) on Pd(111)

Disulfide	ΔE (dissociative adsorption) (eV)	E_{chem} (side-on adsorption mode) (eV)
8a	3.481	n/a
10a	3.102	0.740

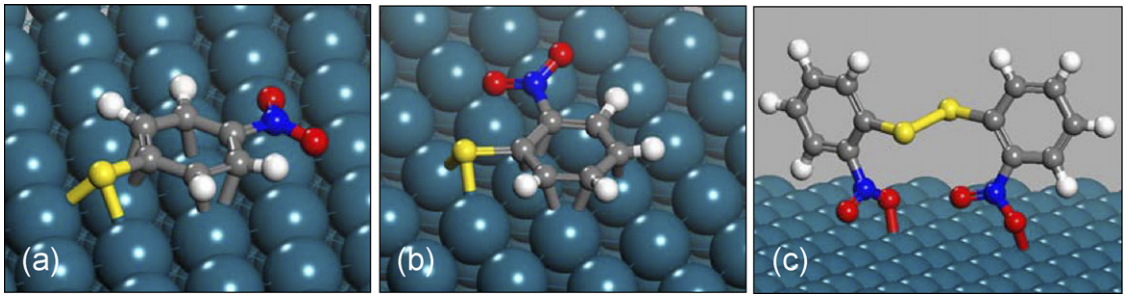

Fig. 6. The optimized monomer adsorption geometries following dissociative adsorption of (a) 4,4′-dinitrodiphenyldisulfide, (b) 2,2′-dinitrodiphenyldisulfide, and (c) the side-on adsorption geometry of 2,2′-dinitrodiphenyldisulfide.

adsorption modes leads to a lower rate of bond cleavage and, consequently, a much lower proportion of **10c**. The production of the 2-aminothiophenol, **10b**, is then limited until sufficient concentration of 2,2′-diaminodiphenyldisulfide, **10d**, has been built up (i.e., pathway B dominates). For **9a**, a mixture of the two pathways is found. Interestingly, at 5 bar the difference between the molecules is less pronounced, possibly indicating that the change in adsorption geometry is favored only at a high surface coverage of hydrogen. At high hydrogen pressures, the side-on adsorption geometry is likely favored, due to competition for surface sites. This effect is analogous to the change in adsorption geometry of benzene over Pd(111) from a flat to tilted state with increasing coverage [32]. At 5 bar, similar reaction pathways are observed for both molecules, due to the fact that both molecules adsorb parallel to the surface and S–S cleavage occurs. At higher pressures, **8a** maintains the flat lying adsorption mode, whereas side-on adsorption becomes more favorable for **10a**, allowing nitro reduction to occur.

Along with sulfur poisoning, inhibition of PGM catalysts can also be caused by nitrogen-containing molecules, particularly amines; for example, Pt or Pd/zeolite catalysts have exhibited decreased tetralin hydrogenation in the presence of NH_3 [10]. On doping the reaction mixture with aminothiophenol, no significant change in either the profile or rate of reaction was observed, demonstrating that the system is resistant to both sulfur poisoning and $–NH_2$ adsorption and that the reaction is not product desorption rate-limited.

To examine the rate-determining step, the reaction was performed at 50 bar for 1 h before the pressure was reduced to 5 bar. The reaction profile after 1 h was as would be expected for a typical reaction performed at 50 bar, with formation of **8c** and **8d**. After the pressure was decreased, **8b** was formed, gradually reaching 50% after 6 h of reaction. In comparison, a reaction performed at 5 bar showed the formation of **8c** and other intermediates, but only trace amounts of **8b** after 6 h (Table 2). This indicates that initiating the hydrogenation of **8c** to **8b** is the slowest step and that once this process begins, the reaction is not sensitive to H_2 pressure. This finding is supported by the fact that if an analogous experiment is performed using the 2,2′-dinitrodiphenyldisulfide, **10a**, which follows predominately pathway B (i.e., nitro reduction then disulfide cleavage), then the reaction does not go on to completion. In this case, the slow cleavage step was performed at the lower pressure, which prevented rapid formation of the 2-aminothiophenol product.

Table 2
Effect of hydrogen pressure on the hydrogenation/hydrogenolysis of **8a** to **8c**

Pressure (bar)	Conversion of **8a** (%)	Yield of **8c** (%)
5	37	4
50	98	100
50–5[a]	99	51

The conversion of **8a** is taken after 1 h of reaction and the yield of **8c** is after 6 h of reaction.
[a] Pressure decreased from 50 bar to 5 bar after 1 h of reaction.

3.4. Hydrogenation/hydrogenolysis of 4,4′-dinitrodiphenyldisulfide in the presence of dimethyldisulfide

Despite the widespread application of dimethyldisulfide (**1a**) as catalyst moderator, rapid hydrogenation occurred under the conditions used in the present study. To investigate the relative adsorption strengths, we hydrogenated **8a** in the presence of **1a** at 5 bar H_2 pressure. The catalyst loading was doubled so that the individual substrate-to-bulk Pd molar ratio remained at 26:1. Fig. 7 compares the initial conversion rates of the substrates. In the presence of **1a**, the rate of conversion of **8a** was unaffected; however, the reaction rate of **1a** was reduced by a factor of ∼22; only when the concentration of **8a** was reduced below 30% was significant conversion of **1a** observed. These results indicate that **8a** was preferentially adsorbed on the surface and almost completely suppressed adsorption of the smaller disulfide. Complete suppression would effectively result in a doubling of the palladium-to-substrate ratio and should increase the rate of reaction. However, the initial rate of the conversion of **8a** was not significantly improved, suggesting that one or more intermediates or the final product strongly adsorbed on the catalyst surface and blocked the additional active sites, hindering the adsorption and subsequent reaction of **1a**.

3.5. Adsorption studies

Although the mass balance for all substrates was found to be ∼100% at the end of the reaction, for the aromatic substrates in particular, a significant variation in balance was observed as a function of reaction time. This is illustrated in Fig. 8 for 4,4′-dinitrodiphenyldisulfide, **8a**. A clear minimum can be seen, due to the retention of the intermediates within the catalyst pores. Comparing the adsorptions of the starting material, intermediates, and product on the carbon support and the catalyst shows that the adsorption was unaffected by the presence of the palladium, as expected from the relative surface areas

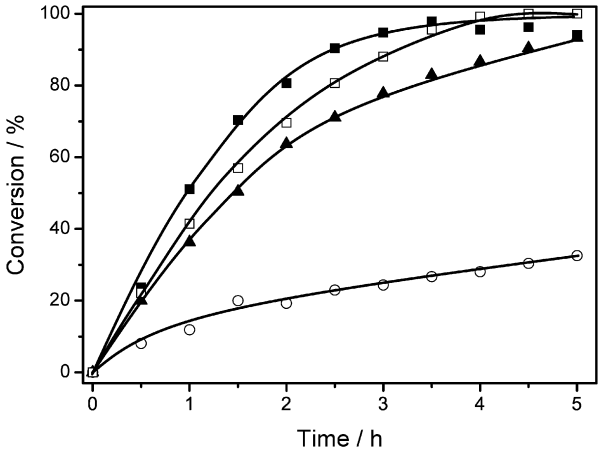

Fig. 7. Comparison of the conversion-time profile for dimethyldisulfide, **1a** (■), and 4,4′-dinitrodiphenyldisulfide, **8a** (▲), as the individual components and in the 1:1 mixture of **1a** (○) and **8a** (□) at 50 bar H_2 at 75 °C in THF using a palladium:substrate ratio of 1:26. The lines are to indicate the trends in the data.

(Fig. 9). Interestingly, the starting material (**8a**) did not adsorb strongly on the surface of either the Pd/C catalyst or the carbon support. This finding agrees with the best-fitted kinetic model, which shows that the reaction is first order with respect to both the substrate and hydrogen pressure for **8a**. This is unusual for catalytic hydrogenation, in which a zero reaction order is normally found for the substrate [33] due to the high surface coverage of the substrate compared with the hydrogen. A higher adsorption constant was found for 4,4′-diaminodiphenyldisulfide **8d** compared with **8a**, due to the more effective hydrogen bonding/chelation of the $–NH_2$ group versus the $–NO_2$ group; however, compared with the cleaved products, both disulfides were weakly adsorbed. Both **8c** and **8b** adsorbed strongly, as was expected due to the presence of the –SH group. Interestingly, in **8b** there was a small but significant variation between the carbon support and the catalyst with the palladium reducing the adsorption constant. Despite the high adsorption of **8b**, clearly (based on the complete mass balance at the end of reaction), other reaction species were present that were not observed in the bulk liquid due to strong adsorption. These eventually converted to **8b**, which desorbed.

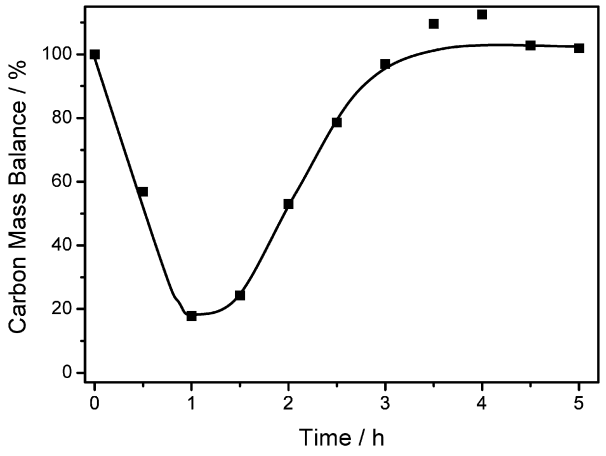

Fig. 8. Variation in the carbon balance as a function of time during the hydrogenation/hydrogenolysis of 4,4′-dinitrodiphenyldisulfide (**8a**) as shown in Fig. 5.

3.6. Recycling

Fig. 10 shows the reaction profile of **8a** at 50-bar hydrogen for the recycled catalyst. Compared with that shown in Fig. 5 for fresh catalyst, that is a clear decrease in the rate of reaction, although a significant level of catalyst activity is maintained. Additional recyclings of the catalyst caused further gradual decreases in the activity of the system; after seven reactions, the rate decreased from 0.62 $\mu mol\,s^{-1}\,m_{Pd}{}^{-2}$ to 0.51 $\mu mol\,s^{-1}\,m_{Pd}{}^{-2}$ at 50 bar H_2 and 75 °C in THF with a palladium-to-substrate ratio of 1:2.6. The same reaction profile was maintained using both the fresh catalyst and the catalyst used in the seventh reaction. Importantly, treatment of the catalyst with flowing hydrogen at 400 °C restored the initial activity.

Powder XRD patterns of the catalyst over seven reactions are shown in Fig. 11. Only peaks consistent with metallic pal-

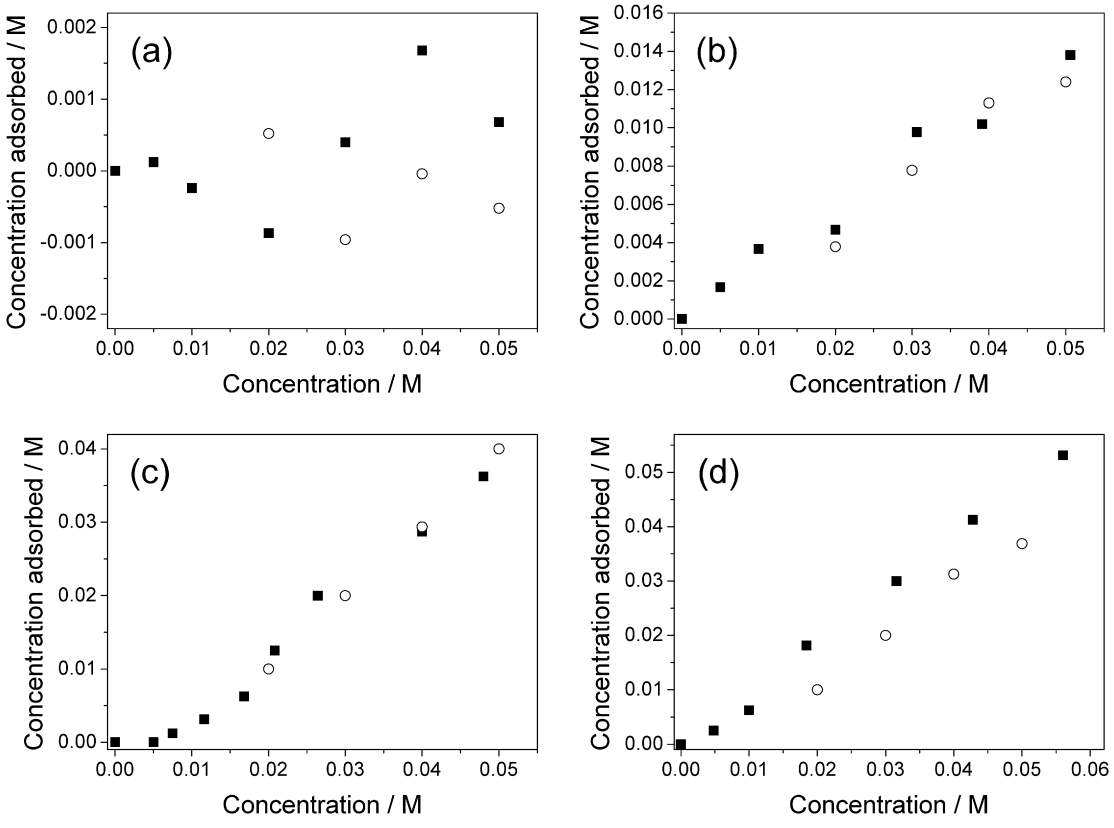

Fig. 9. Adsorption isotherms for (a) 4,4′-dinitrodiphenyldisulfide (**8a**), (b) 4,4′-diaminodiphenyldisulfide (**8f**), (c) 4-nitrothiophenol (**8c**), and (d) 4-aminothiophenol (**8b**) on the Pd/C catalyst (○) and charcoal support (■) stirred over 24 h at 20 °C.

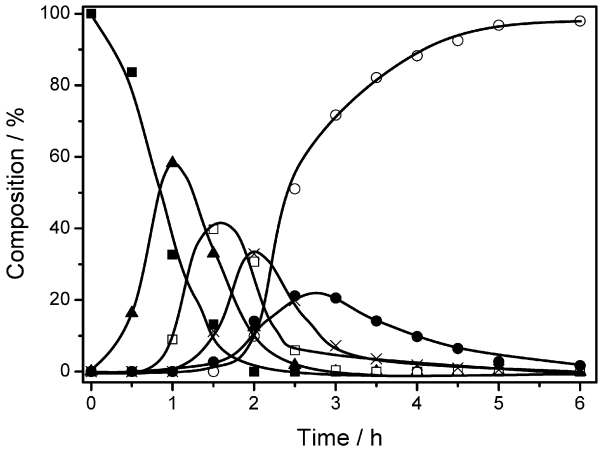

Fig. 10. Reaction-time profile for the hydrogenation/hydrogenolysis of **8a** at 50 bar H_2 and 75 °C in THF with the recycled Pd/C catalyst at a palladium:substrate ratio of 1:26. Herein, the molecules shown by the notation in Fig. 4 are denoted: **8a** (■), **8b** (○), **8c** (▲), **8d** (□), **8e** (●), and **8f** (×). The lines are to indicate the trends in the data.

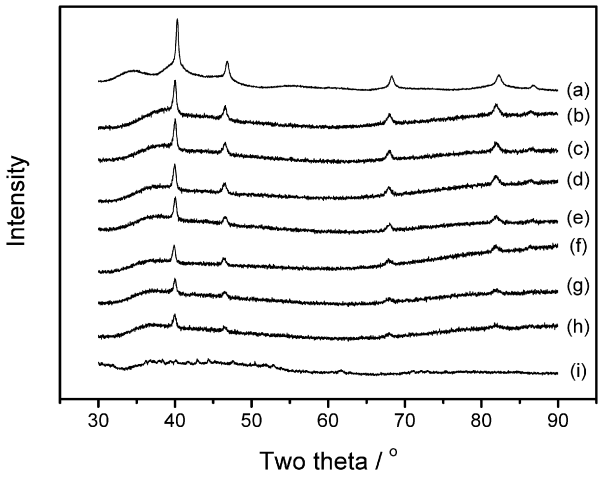

Fig. 11. X-ray diffraction patterns of the Pd/C catalyst (a) prior to reaction and after the (b) first, (c) second, (d) third, (e) fourth, (f) fifth, (g) sixth and (h) seventh hydrogenation/hydrogenolysis reactions of **8a** at 50 bar H_2 and 75 °C in THF with a palladium:substrate ratio of 1:2.6. The trace for the sulfided Pd/C catalyst is shown in (i).

ladium were present in the as-received catalyst and throughout the catalyst recycling; no other peaks appeared. Furthermore, the particle size (as determined by the Debye–Scherrer equation) was maintained at ∼200 Å. A decreased intensity of the palladium peaks occurred with increasing recycle number, as shown in Fig. 12; however, no metal leaching from the catalyst was detected by ICP. The changes in the XRD patterns on recycling can be attributed to the formation of small concentrations of amorphous Pd_xS_y. Similar results were found for all of the substrates examined.

To examine the effect of sulfur poisoning, the catalyst was presulfided by exposing the catalyst to a flow of 15% H_2S in H_2 at 400 °C for 4 h. The subsequent XRD pattern (Fig. 11) shows a complete transformation of the palladium into Pd_4S. The resulting catalyst showed little activity, as expected; for example, in the hydrogenation/hydrogenolysis of **8a** at 50 bar H_2 and 75 °C, <5% conversion was observed, with the formation of only 4-nitrothiophenol even after 24 h. Therefore, the fact that the catalyst maintains a high activity on recycling under the typical reaction conditions is due in part to the fact that no evidence of significant carbon–sulfur bond hydrogenolysis was found in the reaction products. This process could lead to in situ H_2S formation and deactivation of the catalyst.

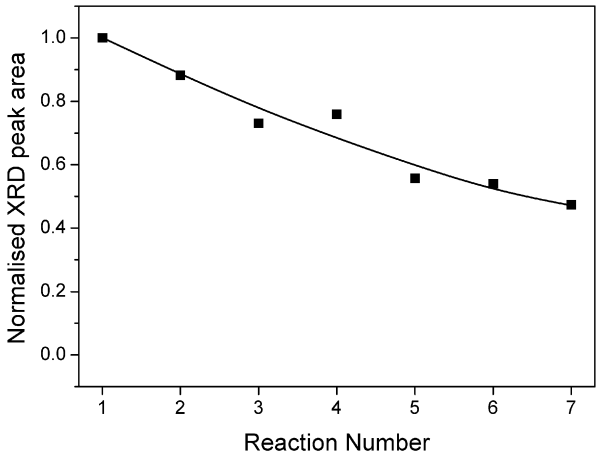

Fig. 12. Normalized area of the palladium X-ray diffraction peak at 40.1° (2θ) as a function of reaction number determined from the traces in Fig. 11.

Palladium sulfide and palladium are known to be good hydrogenation catalysts [34], and thus the nature of the active catalyst under these reaction conditions remains unclear. Although XRD indicated a decrease in the palladium feature (which may be correlated with the loss in activity on recycling), it is also possible that the catalyst surface is sulfided under reaction conditions and that the decreased activity is due to the transformation of an active amorphous surface sulfide (e.g., PdS) into an inactive phase (e.g., Pd_4S).

4. Conclusion

This work reports for the first time the hydrogenation/hydrogenolysis of sulfur-containing molecules over palladium-based catalysts, which is commonly perceived as being impractical due to sulfur poisoning. A range of aliphatic and aromatic disulfides were converted to their corresponding thiols using a Pd/C catalyst. The catalyst retained its structure after the reaction, and only a small decrease in activity was observed on recycling.

The detailed mechanism for the hydrogenation/hydrogenolysis of dinitrodiphenyldisulfides to the corresponding aminothiophenol was examined for *ortho*-, *meta*-, and *para*-substitution patterns. A complex reaction network was observed with two major pathways *via* an initial S–S cleavage or the reduction of the nitro groups. Although both pathways were observed for the substrates, the dominant route was influenced by the proximity of the nitro group to the S–S bond. Cleavage of the S–S follows the order *para*- > *meta*- > *ortho*-substitution and is related to the adsorption geometry of the reactant. For the *para*-substituted reactant, the molecule adsorbs parallel to the surface, whereas for the *ortho*-substituted molecule, the

nitro groups adsorb; the resultant forcing away of S–S from the surface reduces the cleavage rate. The finding that sulfur-containing molecules can be efficiently hydrogenated over palladium-based catalysts without significant loss in activity can extend their use to a new family of substrates.

Acknowledgments

Funding was provided by Johnson Matthey (L.M.) and EPSRC for funding under the CARMAC project.

References

[1] C. Forquy, E. Arretz, Stud. Surf. Sci Catal. 41 (1988) 91.
[2] A. Sakurada, N. Hirowatari, Jpn. patent 8036,409;
A. Sakurada, N. Hirowatari, Jpn. patent 8015,413 (1980) assigned to Mitsubishi Petrochemical Co.
[3] H. Pitt, US patent 2947788 (1960);
H. Pitt, German patent DE 1939468 (1970) to Stauffer Chemical;
K. Fujimori, H. Togo, S. Oae, Tetrahedron Lett. 21 (51) (1980) 4921;
S. Oae, H. Togo, Bull. Chem. Soc. Jpn. 56 (1983) 3802.
[4] E. Knusli, Gazz. Chim. Ital. 79 (1949) 621;
A. Wager, Chem. Ber. 99 (1966) 375;
H. Yamashita, Y. Takahashi, Jpn. patent 7425,255 (1974) to Sugai Chemical Industry Co.
[5] H.C. Brown, B. Nazer, J.S. Cha, Synthesis 6 (1984) 498;
S. Krishnamurthy, D. Aimino, J. Org. Chem. 54 (1989) 4458;
A. Ookawa, S. Yokohama, K. Soai, Synth. Commun. 16 (1986) 819.
[6] L.E. Overman, D. Matzinger, E.M. O'Connor, J.D. Overman, J. Am. Chem. Soc. 96 (1974) 6081;
D.A. Happer, J.W. Mitchel, G.J. Wright, Aust. J. Chem. 26 (1973) 121;
L.E. Overman, S.T. Petty, J. Org. Chem. 40 (1975) 2779.
[7] S.N. Maiti, P. Spevak, M.P. Singh, R.G. Micetich, A.V. Narender Reddy, Synth. Commun. 18 (6) (1988) 575;
S.N. Maiti, M.P. Singh, P. Spevak, R.G. Micetich, A.V. Narender Reddy, J. Chem. Res. Synop. 1 (1988) 256.
[8] C. Calais, M. Lacroix, C. Geantet, M. Breysse, J. Catal. 144 (1993) 160.
[9] C. Calais, M. Lacroix, C. Geantet, M. Breysse, Appl. Catal. A 115 (1994) 303.
[10] T. Matsui, M. Harada, M. Toba, Y. Yoshimura, Appl. Catal. A 293 (2005) 137.
[11] E. Lamy-Pitara, Y. Tainon, J. Barbier, Appl. Catal. 68 (1991) 179.
[12] Z. Pafil, K. Matusek, M. Muhler, Appl. Catal. A 149 (1997) 113.
[13] J.T. Miller, D.C. Köningsberger, J. Catal. 162 (1996) 209.
[14] P. Reyes, G. Pecchi, M. Morales, J.L.G. Fierro, Appl. Catal. A 163 (1971) 145.
[15] J.A. Rodriguez, M. Kuhn, J. Phys. Chem. 99 (1995) 9567.
[16] H. Chu, W.T. Lee, K.H. Horng, T.K. Tseng, J. Hazard. Mater. B 82 (2001) 43.
[17] J.-R. Chang, S.-L. Chang, T.-B. Lin, J. Catal. 169 (1997) 338.
[18] A. De Sarkar, B.C. Khanra, J. Mol. Catal. A 229 (2005) 25.
[19] P.A. Gravil, H. Toulhoat, Surf. Sci. 430 (1999) 176.
[20] L.J. Hoyos, M. Primet, H. Praliaud, J. Chem. Soc. Faraday Trans. 88 (1992) 113.
[21] N. Pernicone, M. Cerboni, G. Prelazzi, F. Pinna, G. Fagherazzi, Catal. Today 44 (1998) 129.
[22] K. Ito, T. Tomino, M. Ohshima, H. Kurokawa, K. Sugiyama, H. Miura, Appl. Catal. A 249 (2003) 19.
[23] V.R. Choudhary, M.G. Sane, J. Chem. Technol. Biotechnol. 73 (1998) 336.
[24] E.B. Maxted, Adv. Catal. 3 (1951) 129.
[25] G.J. Hutchings, F. King, I.P. Okoye, C.H. Rochester, Appl. Catal. A 83 (1992) L7.
[26] P.C. l'Argentiere, N.S. Figoli, Appl. Catal. 61 (1990) 275.
[27] D. Sanchez-Portal, P. Ordejon, E. Artacho, J.M. Soler, Int. J. Quantum Chem. 65 (1997) 453;
J.M. Soler, E. Artacho, J.D. Gale, A. Garcia, J. Junquera, P. Ordejon, D. Sanchez-Portal, J. Phys. Condens. Matter 14 (2002) 2745.
[28] N. Troullier, J.L. Martins, Phys. Rev. B 43 (1991) 1993.
[29] J.P. Perdew, K. Burke, M. Ernzerhof, Phys. Rev. Lett. 77 (1996) 3865.
[30] E. Lamy-Pitara, Y. Tainon, J. Barbier, Appl. Catal. 68 (1991) 179.
[31] G.C. Bond, Platinum Met. Rev. 12 (1968) 100.
[32] A.F. Lee, K. Wilson, R.M. Lambert, A. Goldoni, A. Baraldi, G. Paolucci, J. Phys. Chem. B 104 (2000) 11729, plus references therein.
[33] H.A. Smith, W.C. Bedoit, J. Phys. Colloid Chem. 55 (1951) 1085.
[34] For example, A. Ermakova, A.V. Mashkina, L.G. Sakhaltueva, Kinet. Catal. 43 (2002) 528.